

Confirmation of anomalous dynamical arrest in attractive colloids: A molecular dynamics studyE. Zaccarelli,¹ G. Foffi,^{1,2} K. A. Dawson,² S. V. Buldyrev,³ F. Sciortino,¹ and P. Tartaglia¹¹*Dipartimento di Fisica, Istituto Nazionale di Fisica della Materia, and INFM Center for Statistical Mechanics and Complexity, Università di Roma La Sapienza, Piazzale Aldo Moro 5, I-00185 Rome, Italy*²*Irish Centre for Colloid Science and Biomaterials, Department of Chemistry, University College Dublin, Belfield, Dublin 4, Ireland*³*Center for Polymer Studies and Department of Physics, Boston University, Boston, Massachusetts 02215*

(Received 21 June 2002; published 21 October 2002)

Previous theoretical simulation and experimental studies have indicated that particles with a short-ranged attraction exhibit a range of dynamical arrest phenomena. These include very pronounced reentrance in the dynamical arrest curve, a logarithmic singularity in the density correlation functions, and the existence of “attractive” and “repulsive” glasses. Here we carry out extensive molecular dynamics calculations on dense systems interacting via a square-well potential. This is one of the simplest systems with the required properties, and may be regarded as canonical for interpreting the phase diagram, and now also the dynamical arrest. We confirm the theoretical predictions for reentrance, logarithmic singularity, and give a direct evidence of the existence, independent of theory, of two distinct glasses. We now regard the previous predictions of these phenomena as having been established.

DOI: 10.1103/PhysRevE.66.041402

PACS number(s): 82.70.Dd, 64.70.Pf, 83.10.Rs, 61.20.Ja

I. INTRODUCTION

Recently, there has emerged a series of remarkable results involving the dynamical arrest of particles with interaction potentials that are short compared to the size of the repulsive core [1–9]. The most important predictions are as follows [10]. The curve at which the fluid phase is arrested is reentrant in the regime where attractions and repulsions compete. In the vicinity of this reentrance, and in the arrested regime, there exist two distinct arrested states that may, under some conditions, coexist. These two states differ in their long-term dynamics. This coexistence terminates smoothly, the dynamics of the two arrested states becoming identical at a particular point at which distinctive dynamics is expected. It is important to note that all these phenomena are predicted to occur irrespective of the shape of the potential (explicit results exist for square-well or hard-core Yukawa interaction models [4–7,11], as well as for the Baxter model [12] despite its singular behavior at the hard-core value [2,3]). The essential feature is only that the range of the attraction in comparison to the hard core must be extremely small.

The results described above were first deduced from the mode-coupling theory (MCT) [13,14], and we may note that the conclusions do not depend on the details of the approximation for the input static structure, Percus-Yevick, mean spherical, and self-consistent Ornstein-Zernike approximation, all leading to essentially the same picture. Within MCT the merging of the two arrested states is predicted to be a higher order dynamical singularity, and density correlations in its vicinity are expected to obey a highly distinctive logarithmic relaxation [4,15], in contrast to the conventional ergodic-nonergodic transition, where a two-step process takes place [14,16].

More recently, this decay has been observed also in several experimental systems [17–19,9,20], thus giving the first evidence that these singularities do exist in nature.

Two recent numerical works [8,21] have focused on the new dynamical features characterizing attractive colloidal

systems. In Ref. [8], colloidal interactions were modeled with a potential chosen in such a way to avoid undesired effects such as liquid-gas separation at low densities. Polydispersity was included to prevent crystallization at high densities. In Ref. [21] molecular dynamics simulations of a square-well (SW) system with a very narrow range of attraction have been performed. In both cases, the results have been shown to be in excellent agreement with MCT predictions. The focus on the simple square-well potential makes direct contact both with the available theoretical results and with experimental systems, the interactions being completely controllable and independent of external parameters. For the SW model, a theoretical solution is also available. Indeed, the equilibrium properties of the square-well potential have been studied for many years, and in many ways it is regarded as the simplest physical model that exhibits all the essential features of short-ranged systems [22–27]. Besides this, it is the model for which the theory of the dynamical arrest transition described above has been developed [4,5] and for which, therefore, detailed comparison may be made between theory and simulation. It may therefore be regarded as canonical in this arena of study.

In Ref. [21], we examined a one-component square-well system. We found that, irrespective of the sharp intervening of crystallization, which effectively prevented the system to approach very closely the glass transition, it was possible to have a clear picture of the reentrant shape of the glass curve in the temperature-density plane. This was achieved by plotting isodiffusivity curves and examining their trends when approaching the limit $D \rightarrow 0$. The shape of the liquid-glass line was found to be in good agreement with the previous MCT predictions [4].

In this paper, we report an extensive numerical study of a two-component binary mixture with interactions modeled by a very narrow SW potential. This mixture appears to be a logical extension of the one-component system [21] for which crystallization is effectively avoided, by means of the geometrical rearrangements allowed by the asymmetry in di-

ameters between particles of different species. The choice of a two-component system makes it possible to extend the range of isodiffusivity curves to almost 3 decades [28], as well as the range of studied packing fractions from ≈ 0.57 for one-component to 0.62 for binary systems. Thus, the re-entrance is so pronounced that an equivalent hard-sphere system at this highest packing fraction value, i.e., 0.62, would be sufficiently dense to approach the random-close-packed limit, though the definition of that concept has its own limitations [29].

The extension to a binary system does not only make more evident the reentrant behavior of the glass transition curve, but also allows a deeper study of the dynamics of the system. Indeed, as one can approach much more closely the ideal glass line, intended as the $D \rightarrow 0$ locus of the (ϕ, T) plane, the influence of higher order MCT singularities on the dynamics becomes much more evident. We know from theoretical work that the 3% case of the square-well model possesses indeed an A_3 singularity [4,5], corresponding to the end point of the repulsive-attractive glass-glass transition. Though, of course, this singularity lies inside the glassy region, its presence is signalled by the characteristic logarithmic decay of density correlators mentioned above, already in the liquid region, when going sufficiently close to the neighboring glass boundary.

We report in this paper a characteristic behavior of the density correlators, near the ideal glass transition, which combines features of the typical A_2 singularity, i.e., simply ergodic to nonergodic transition with a two-step power-law relaxation, and of higher order singularities associated with logarithmic decay. This produces, in a certain region of the (ϕ, T) plane, a behavior that is originated by a competition between the two types of MCT solutions. The same kind of interesting result is found in the mean-square displacement (MSD). However, this subtle interplay between different singularities is present also in theory [4,15], and its manifestation in simulation should be regarded as support for the theory, rather than an inconvenience. This will allow us to identify and localize quite clearly a genuine MCT higher order singularity in a realistic model.

II. SIMULATION AND THEORY

We study binary mixtures of SW spheres. In particular, we focus on samples of a 50%-50% mixture of $N=700$ spheres in a cubic box, with the diameter ratio between the two species equal to 1.2. Thus, the smaller particles' (B -type) diameter is $\sigma_B=1$, and both A and B particles have unit mass. Both species interact with a square-well potential with the ratio between the potential range and particle diameter equal to 3%. This corresponds to one of the cases studied theoretically within MCT, which clearly possesses all the main phenomena [4,5,30]. The 3% ratio has been chosen also for interactions between particles of different species, i.e., we consider

$$V_{ij}(r) = \infty \quad r_{ij} < \sigma_{ij},$$

$$V_{ij}(r) = -u_0 \quad \sigma_{ij} < r_{ij} < \sigma_{ij} + \Delta_{ij},$$

$$V_{ij}(r) = 0 \quad r_{ij} > \sigma_{ij} + \Delta_{ij}, \quad (1)$$

with $\epsilon_{ij} = \Delta_{ij}/(\sigma_{ij} + \Delta_{ij}) = 0.03$, $i, j = A, B$ and we use the conventional notation for which, for example, $\sigma_{AA} = \sigma_A$ and $\sigma_{AB} = (\sigma_A + \sigma_B)/2$. Temperature T is measured in units of energy, i.e., $k_B = 1$ and thus, for example, $T=1$ corresponds to average thermal energy per particle being equal to $3/2$ of the well depth, while the packing fraction is defined as $\phi = (\rho_A \sigma_A^3 + \rho_B \sigma_B^3)(\pi/6)$, where $\rho_i = N_i/L^3$, L being the box size and N_i the number of particles for each species.

Initial configurations for each density were chosen at random. Particles were separated in successive steps—with more particular care, the higher the density of interest—to implement the hard-core repulsion. When separation was ensured, the attractive well was added. To reach the temperature of the study, the configuration so prepared was then left to evolve with a thermostat of constant thermal coefficient for a period of time sufficient to equilibrate at that temperature. We estimate the equilibration time as the time at which the density correlation function of the slowest collective mode (i.e., at the structure factor peak) has decayed to zero. After this equilibration, the configuration was left to run at constant energy for a time dependent on the slowness of the dynamics, for a time covering at least ten equilibration times.

Simulation time is measured in units of $\sigma_B(m/u_0)^{1/2}$. The standard molecular dynamics algorithm has been implemented for particles interacting with SW potentials [31]. Between collisions, particles move along straight lines with constant velocities. When the distance between the particles becomes equal to the distance for which $V(r)$ has a discontinuity, the velocities of the interacting particles instantaneously change. The algorithm calculates the shortest collision time in the system and propagates the trajectory from one collision to the next one. Calculations of the next collision time are optimized by dividing the system in small subsystems, so that collision times are computed only between particles in the neighboring subsystems.

We studied eight isothermal cuts of the phase diagrams, with the temperature varying between 2.0 and 0.3 in the large packing fraction region, i.e., $\phi > 0.5$. In addition, we examined the hard-sphere case, where no attractive interactions are present. For each considered configuration, we first studied the thermal history to check that, effectively, it maintains itself at the required temperature within fluctuations and that the total energy remains constant.

Of each studied configuration, we considered the time-dependent density correlation functions for different q vectors to make a direct comparison with the behavior predicted by MCT. The correlators for each species of particles, i.e., $i \neq j$, are defined as

$$\phi_{ij}(q, t) = \frac{S_{ij}(q, t)}{S_{ij}(q)} = \frac{\langle \rho_i(-q, t) \rho_j(q, 0) \rangle}{\langle \rho_i(-q, 0) \rho_j(q, 0) \rangle}, \quad (2)$$

where $\rho(\mathbf{q}, t) = \sum_l \exp[i\mathbf{q} \cdot \mathbf{r}_l(t)]$ are the density variables for each species and $S_{ij}(q)$ are the partial static structure factors of the system. The $\phi_{ij}(q, t)$ are the fundamental quantities of

interest in the mode-coupling theory, which consists of writing a set of generalized Langevin equations, which can be closed within certain approximations [13,14,32,33].

We note here that colloidal systems exhibit a Brownian short-time dynamics, while our simulations obey a standard Newtonian dynamics. This will result in the presence of a ballistic short-time regime for the mean-squared displacement. However, a crucial result of MCT is that the structural relaxation dynamics, i.e., the dynamics outside the transient, is independent of the short-time dynamics [34].

The correlators $\phi_{ij}(q,t)$ have been calculated by averaging over several independent configurations and over up to 100 different wave vectors with the same modulus, to obtain a good statistical sample. Interesting behavior of these observables arises when the dynamics of the system gets slower, i.e., where the dynamical behavior is of the “supercooled” type, even though for the present system we do not know the exact location in the control parameter space of the melting point. What follows is what is commonly observed for the density correlators and diffusivity behavior of a supercooled fluid, which is approaching the dynamical arrest. Indeed, in this particular regime, one finds the typical two-step relaxation shape for the density correlators, which is an indication of the emergence of two distinct timescales in the structural relaxation of the system. A first relaxation process, the so-called β relaxation, occurs at short times, and it is due to particles exploring the cages formed by their nearest neighbors. On the other hand, a second process, the α relaxation, occurs at larger and larger time scales, the slower the dynamics, originating the formation of a longer and longer plateau region. This accounts for the restoration of the ergodicity in the system, where particles have been able to escape from their cages and explore larger portions of phase space. At the ideal glass transition, the time of the α relaxation is predicted to diverge, and the correlators do not relax anymore, thus reaching a finite plateau value. This is defined as the nonergodicity parameter $f_{ij}(q) = \lim_{t \rightarrow \infty} \phi_{ij}(q,t)$, which jumps discontinuously from zero to a finite (critical) value $f_{ij}^c(q)$ at the transition, signalling the occurrence of an ergodic (fluid) to nonergodic (glass) transition. This picture of the dynamical correlators is found to be in excellent agreement with experimental and simulation results, though in real systems the α -relaxation time does not diverge, but only becomes increasingly larger. This is due to the intervening of other processes, commonly termed as “hopping” processes, which restore ergodicity, and are not included in the MCT treatment for the ideal glass transition described above.

The two-step relaxation is well described by MCT, through an asymptotic study of the correlators near the ideal glass solutions. The approach to the plateau is described by a power law, regulated by the exponent a , i.e.,

$$\phi_q(t) - f_q^c \sim h_q^{(1)}(t/t_0)^{-a} + h_q^{(2)}(t/t_0)^{-2a} \quad (3)$$

with t_0 the microscopic time, while the departure from the plateau, i.e., the start of the α process, is expressed in terms of another power law, regulated by the exponent b ,

$$\phi_q(t) - f_q^c \sim -h_q^{(1)}(t/\tau)^b + h_q^{(2)}(t/\tau)^{2b} \quad (4)$$

with τ the characteristic time of the relaxation. The exponents a and b are related to each other with a transcendental relation, and are independent of the particular q vector considered, $h_q^{(1)}$ and $h_q^{(2)}$ are referred to, respectively, as the critical amplitude and correction amplitude [14].

On the other hand, the α -relaxation process can be also well described by a stretched exponential, i.e.,

$$\phi_q(t) = A_q \exp[-(t/\tau_q)^{\beta_q}], \quad (5)$$

where the amplitude A_q determines the plateau value, and the exponent β_q is always less than 1.

We can thus fit the correlators, for each q value considered, both in terms of the MCT prediction and of the stretched exponential, and find an estimate of the nonergodicity factor f_q as a function of q . The shape of this quantity can be indicative of the formation of different types of glasses, either attractive or repulsive dominated [1,2,4,5].

However, what we have described so far is typical for A_2 singularities. These correspond to the simplest nontrivial solutions for the nonergodicity parameter MCT equations, and, for example, in the hard-sphere model only this type of singularity can arise. This is due to the fact that the only control parameter of the model is the packing fraction. When the number of control parameters increases, higher order singularities may occur. For a square-well model it was shown that singularities of types A_3 and A_4 are present within the theory [4] when the width of the well becomes much smaller than the hard-core radius. In the proximity of such singularities, the asymptotic behavior for the density correlators is different from the one we have seen so far [4,15]. In particular, we have for the leading contribution a logarithmic behavior,

$$\phi_q(t) - f_q^c \sim -C_q \ln(t/\tau). \quad (6)$$

Higher order corrections to this behavior can be calculated through an asymptotic expansion of the MCT equations close to the singularities and they are found to be crucial for some predictions, as discussed in Ref. [15].

Another main focus of our study was to evaluate the MSD $\langle r^2(t) \rangle$ of particles with respect to their initial positions. Typically, the behavior of the MSD at short times follows the simple law $\langle r^2(t) \rangle \sim t^2$, which accounts for the ballistic motion of the particles, i.e., particles move freely without collisions. At later times, particles start to feel the presence of each other and there is a crossover to the diffusive regime, i.e., $\langle r^2(t) \rangle \sim t$. The proportionality constant of this relation defines the diffusivity D of the system, via the celebrated Einstein relation [35]

$$\lim_{t \rightarrow \infty} \frac{\langle r^2(t) \rangle}{t} \simeq 6D. \quad (7)$$

Thus, by evaluating the long-time limit of the MSD, we determine the diffusion coefficient D for each state point.

Though this general behavior is preserved, when the dynamics becomes slower, a crossover region between short and late times emerges. Of course, the duration of this intermediate region increases, the slower the dynamics. This phe-

nomenon is the corresponding behavior for the MSD of the separation of the two time scales that we have seen in the correlation functions. It also reflects the formation of cages in which particles get trapped, so that diffusion becomes more difficult. The crossover region consists generally in the development of a plateau also for the MSD. At the ideal glass transition, the α -relaxation time would diverge, and diffusion from the plateau would not occur even at infinite times, in complete analogy with the correlators behavior. Thus, the height of the plateau is related to the localization length of particles in the arrested state, i.e., the size of the cages of the glass. Of course, in simulations, only finite times can be explored and the position of the ideal glass transition can be only extrapolated by data.

As for the correlators, the presence of higher order singularities may affect the plateau region of MSD, giving rise to peculiar behavior.

MCT predicts a power-law decrease for the diffusivity on approaching the ideal glass transition. Along an isotherm,

$$D \sim |\phi - \phi_c|^\gamma, \quad (8)$$

where ϕ_c is the value of the packing fraction at the transition (“critical” value), i.e., the value where the diffusivity would drop to zero for the considered temperature. The exponent γ is completely determined by the theory in terms of the exponents a and b , defined in Eqs. (3) and (4), via the simple relation [14]

$$\gamma = \frac{1}{2a} + \frac{1}{2b}. \quad (9)$$

Also the so-called exponent parameter λ is related to these exponents via the relation

$$\lambda = \frac{\Gamma(1+b^2)}{\Gamma(1+2b)} = \frac{\Gamma(1-a^2)}{\Gamma(1-2a)}. \quad (10)$$

Thus, only one of the parameters is, in principle, sufficient to determine all the others. However, the parameter λ is the crucial one in determining the presence of higher order singularities [4], in particular, it tends to the value $\lambda=1$ at an A_3 point, while for a simple A_2 singularity it is always less than 1 [36,14]. Thus, for example, an increase of λ along the A_2 glass line indicates a closer proximity to the A_3 singularity [4].

To summarize, the procedure we use to determine the exponents, and consequently the location of the MCT singularities in the control parameter space, as well as the nonergodicity parameter, is as follows. From fitting the diffusivity behavior at constant temperature with Eq. (8), one can determine the exponent γ , and from this also a , b , and λ . Thus, with the obtained value of b , one can perform a fit of the density correlators, using Eq. (4), and determine the nonergodicity parameter consistently.

However, close to higher order singularities, we do not expect that this behavior is generally preserved, as the logarithmic behavior in the correlators and the transient region in the MSD intervene. Indeed, in these conditions, the exponent b tends to zero (thus originating the logarithmic behavior)

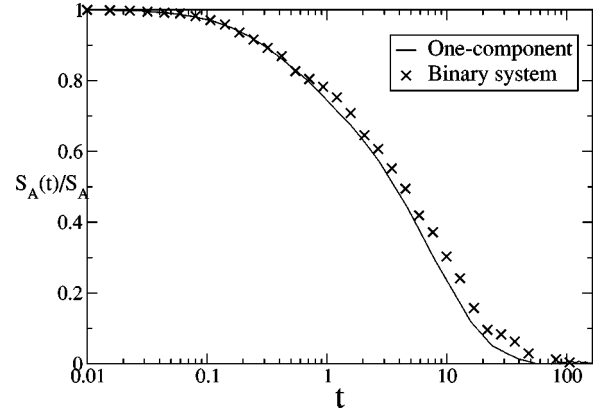


FIG. 1. Comparison between the density-density correlation function $S_{AA}(q^*, t)/S_{AA}(q^*)$ in the binary and the monodisperse case at $\phi=0.57$ and $T=0.75$, corresponding to the most reentrant point found in the monodisperse case, before crystallization intervenes. The wave vector chosen corresponds for both cases to $q^* = 2\pi/\sigma_A$.

and, from the relation between b and γ , one can see that γ would go to ∞ , thereby rendering Eq. (8) meaningless to describe the arrest. Thus, the region of validity of the asymptotic predictions may shrink significantly close to higher order singularities.

III. RESULTS: THE OVERALL PICTURE

The considered mixture represents a natural extension of the monodisperse system studied so far [21]. Indeed, the small asymmetry in diameter does not produce a significant change in the dynamics of the two cases, and, on the contrary, allows to reach much larger packing fractions with no sign of crystalline order. The first of the two statements can be explained by looking at Fig. 1. Here, we compare the behavior of density correlators at a corresponding point on the control parameter space of the system. For the monodisperse case, we are almost at the most reentrant point before crystallization takes place, i.e., $\phi=0.57$ and $T=0.75$. We can clearly see that dynamics does not appear to be particularly slowed down. To make the comparison with the binary case, we are considering the total density correlation function for the species 1 at the q vector, corresponding approximately to the first peak of the static structure factor, and the quantities have been rescaled in order to compare particles with equal diameters. It is evident that the dynamical behaviors are very close; thus in this sense, we can think of carrying out an extension of the one-component work.

In the following, we will focus on the properties of particles of type A. Thus all quantities reported without label, will refer to them. This choice derives from the fact that we do not expect substantial differences in the behavior of the two species, due to the small amount of asymmetry in their sizes.

We start by comparing the T and ϕ dependences of the diffusion coefficient. The diffusion coefficients can be normalized with respect to the factor $D_0 = \sigma_A \sqrt{T/m}$, which takes into account the T dependence of the microscopic time.

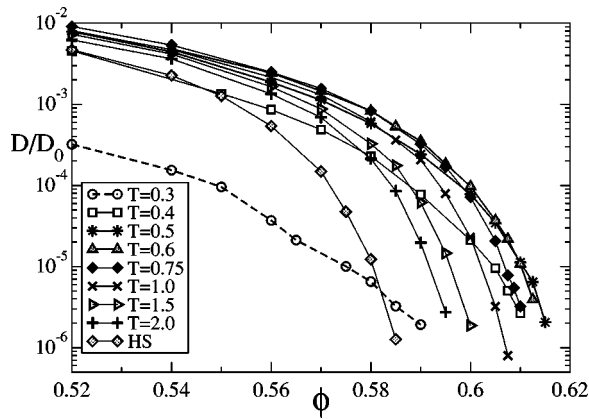


FIG. 2. Normalized diffusion constant D/D_0 , with $D_0 = \sigma\sqrt{T/m}$ as a function of packing fraction ϕ , along each studied isotherm between $T=0.3$ and $T=2.0$. The normalization factor takes into account the difference due to different initial velocities, and ensures the common low density limit (see Ref. [21]).

This ensures that the difference in the average velocities due to the temperature is eliminated, and the diffusion can be considered to be comparable between different temperatures.

A plot of D/D_0 as a function of packing fraction, along the considered isotherms, is shown in Fig. 2. In the present work, we focus our attention mainly on the high density regime, i.e., $\phi > 0.5$. The behavior of the diffusivities presents many similarities with the case of a monodisperse sample of SW spheres [21]. However, striking features appear due to the fact that, for the chosen binary system, it is possible to reach diffusivities three orders of magnitude smaller than in the monodisperse case, as well as much larger packing fractions with no sign of crystallization.

We present results of normalized diffusivities varying roughly between 10^{-2} and 10^{-6} , while the monodisperse system could only reach values of the order 10^{-3} [28], due to the intervening of crystallization [21]. We remark that here the lowest diffusivity values were imposed by computational times, and not by crystallization, as in the monodisperse case. Also, the attractive binary system is able to occupy effectively a larger amount of available volume, thus reaching liquid states up to a packing of about 0.62. On the other hand, the hard-sphere case reaches comparable values of diffusivities at a packing fraction of about $\phi = 0.585$ (see Fig. 4), a value close to that experimentally established for the one-component hard-sphere case [37].

Examining the figure, it is evident that the behavior of the diffusivity is driven by two competing mechanisms. Upon decreasing temperature, starting from the highest value, the presence of the repulsive core, initially dominant, enters in competition with the attractive interactions. This is manifested in the diffusion getting larger, at the corresponding packing fraction, when the temperature gets lower. In other words, the system reaches the same diffusivity at larger and larger packing fractions. This is due mainly to the geometrical rearrangement of particles, i.e., the particles tend to get closer due to the lower temperature, thus producing more available space for the diffusion of the system. However, when the temperature becomes small enough, i.e., effectively

lower than the energy scale of the square well, attractions become dominant and, thus, diffusion becomes slower again because particles tend to remain within each other's shell of attraction.

We know from theoretical calculations within the MCT that this phenomenon is typical of very narrow attractive potentials, both for square-well interactions [4] and for hard-core Yukawa [6]. Indeed, the 3% choice for the range of the attractive well in our simulation is chosen to ensure that the competition between attraction and repulsion is particularly sharp. This can be explained in terms of cages, i.e., when the attractive range is not small enough, which means few percents of the diameter; there is not much difference between cages formed by neighboring particles at high or low temperatures. On the other hand, a very localized attraction can effectively change the shape of the cages, by sticking particles within the well distance Δ . This produces the larger diffusions observed at intermediate temperatures, when the two mechanisms almost balance each other. Similarly, extremely short-ranged attractions produce a solid-solid isostructural transition between an attractive-dominated and a repulsive-dominated crystal [38]. This has been correlated with the glass-glass transition predicted by MCT in a recent work [6]. Of course, it would be interesting to extend the simulations to different values of the range of the potential to confirm the width dependence of the anomalous behavior.

Observing more carefully Fig. 2, the two mechanisms of diffusion produce two different trends of behavior for the plotted curves. Indeed, for $T > 0.6$ the curves present a quite dramatic decrease of diffusivity, while for smaller temperatures the same decrease of about four orders of magnitude occurs on a much wider range of packing fractions (for example, comparing $T=2.0$ and $T=0.4$, the range almost doubles).

We also note that if we plot the bare diffusion coefficients, as evaluated from the fit of the MSD, without normalizing by D_0 , the reentrant behavior is preserved. This can be an advantage, from an experimental point of view, because it would allow us to observe, at the same packing fraction for various temperatures, the diffusivity first increasing then decreasing again, without having to include the thermal factor. We plot in Fig. 3 the unnormalized diffusivities at fixed packing fractions, varying the temperature. The appearance of a maximum, sharper with increasing density, is indeed another manifestation of the reentrance. Extracting the values of maximum diffusivity, it is possible to draw a "maximum diffusivity" line on the (ϕ, T) plane. Note that a different type of diffusivity anomaly occurs in some complex systems such as water, in which diffusivity has a maximum with respect to density at constant T . This anomaly plays an important role in the understanding of the metastable part of the water phase diagram [39].

To make contact with the theoretical results for the ideal glass transition, we have extrapolated curves of normalized isodiffusivities, as for the monodisperse case [21], and represented them in Fig. 4. Of course, the limit $D \rightarrow 0$ would correspond to the ideal glass line, as calculated by MCT. We report the curves for normalized values varying between 5×10^{-3} and 5×10^{-6} , and in the inset we present for com-

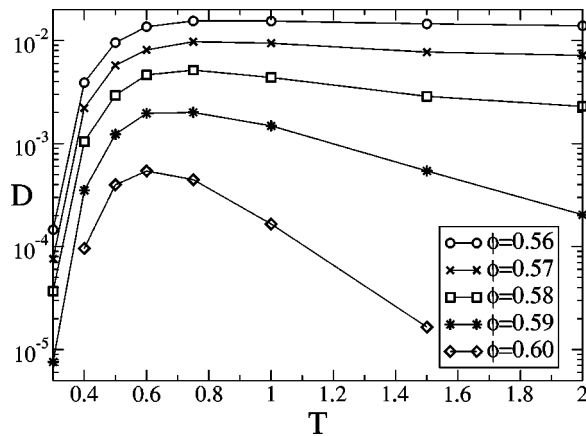


FIG. 3. As in Fig. 2 but, in this case, the diffusion constant has not been normalized, and it is plotted against temperature along isochores between $\phi = 0.56$ and $\phi = 0.60$. The maximum in the bare diffusivity becomes more evident (almost two orders of magnitude) as one moves in the more reentrant part of the (ϕ, T) plane.

parison the ideal glass line as predicted by MCT for a SW one-component system.

It is interesting to comment on the behavior of the iso-diffusivity curves. Depending on which diffusivity value is chosen, the most reentrant point, i.e., the (ϕ, T) point characterized by the largest packing fraction with that diffusivity, changes. In the considered range of diffusivities, its temperature varies from 0.75, which also corresponds to the most reentrant point for the monodisperse case, to 0.5. However, the data of Fig. 2 allow to say that, in the limit $D \rightarrow 0$, such a point will be found at a finite temperature between 0.4 and 0.5, since the attained packing fractions are so large that it would not be possible, within the trend, to go much beyond.

The reentrant behavior, present in mode-coupling calcula-

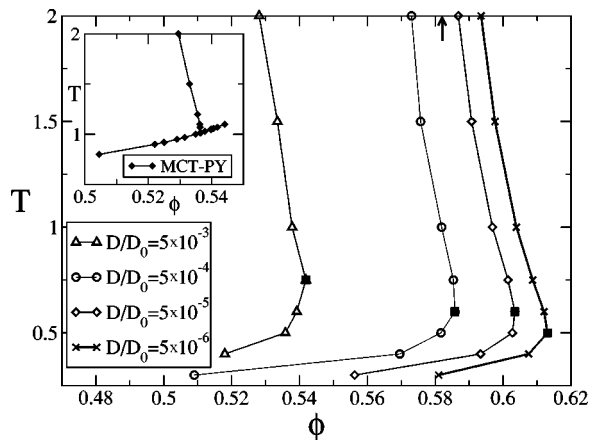


FIG. 4. Curves of iso-normalized-diffusivity D/D_0 in the (ϕ, T) plane. We indicate with a vertical arrow the location for the hard-sphere case of the packing fraction ($\phi \sim 0.582$) for the lowest iso- D/D_0 curve, i.e., $D/D_0 = 5 \times 10^{-6}$. Along each curve, the corresponding most reentrant point is represented with a filled squared symbol, to help the reader follow the description in the text. The inset shows the MCT prediction, calculated in Ref. [4], with the structure factor obtained using the Percus-Yevick approximation as input.

tions, is then confirmed by simulation. It is clear that, since MCT overestimates the effect of packing, we should not expect a perfect quantitative agreement between theory and numerical results. Indeed, for example, for the simple hard-sphere case, the MCT critical glass transition packing fraction is $\phi \approx 0.516$ [13,40], whereas in experiments this has been shown to be $\phi \approx 0.58$ [37]. On the other hand, the same experiments have shown that more accurate predictions can be expected for the behavior of dynamical quantities such as the density-density correlation functions and the MSD.

IV. RESULTS: DYNAMICS ALONG ISOTHERMS

We start by examining the results for the isotherm $T = 2.0$. Here particles have sufficient thermal energy to escape the attractions, and the resulting dynamics appears to be quite similar to that expected for ordinary hard spheres. However, the effect of the attraction, though not changing the general behavior, is to enlarge the liquid part of the phase diagram toward packing fractions already quite larger than the typical (one-component) hard-sphere value, i.e., 0.58. At this temperature, indeed, the system behaves as a fluid at least up to a packing fraction $\phi = 0.595$, where the time limit of our simulation is reached. Close to this limit value, the diffusivity decreases by almost two orders of magnitude for a variation of 1% in the packing fraction.

In Fig. 5(a) we report the time-dependent density-density correlators for different packing fractions, up to the closest to the ideal glass transition. The dramatic decrease in diffusivity is reflected in the behavior of the correlators by the formation of the typical two-step relaxation process near the arrest, described above. Similar behavior can be also observed in the behavior of the MSD displayed in Fig. 5(b). We note, however, that the height of the plateau of $\approx 10\%$ of the particles' diameter is consistent with Lindemann's melting criterion [41,13]. We note here that the density correlators, both for this temperature and for the ones we will discuss later, do not show strong oscillations at short times, differently from what is commonly obtained from simulations of Lennard-Jones systems [42]. This could depend on the presence of the hard core in the potential, which acts as a strong damping term in the short-time dynamics [43].

The diffusivity data can be fitted with the MCT power-law behavior [Eq. (8)]. This holds sufficiently close to the ideal glass transition, thus we considered relevant for the fit only those points for which a clear α -relaxation process was evident. Doing so, we found $\gamma \approx 3.2 \pm 0.4$, and an indication of the quality of the fit is shown in the inset of Fig. 5(b) (see figure caption for details). We note that, getting close to the transition packing fraction, it seems that there are no strong corrections to the power-law behavior, at least in our window of observation. This seems to suggest, as expected, that in colloidal systems with a hard-core potential, hopping effects are less relevant than in atomic systems.

The obtained value for γ is already much larger than the typical one-component hard-sphere value predicted by MCT, i.e., $\gamma^{HS} = 2.58$ [40]. In the case of our particular binary mixture, in the hard-sphere case, whose diffusivity behavior is also reported in Fig. 2, we found a value of $\gamma = 2.9 \pm 0.2$. The

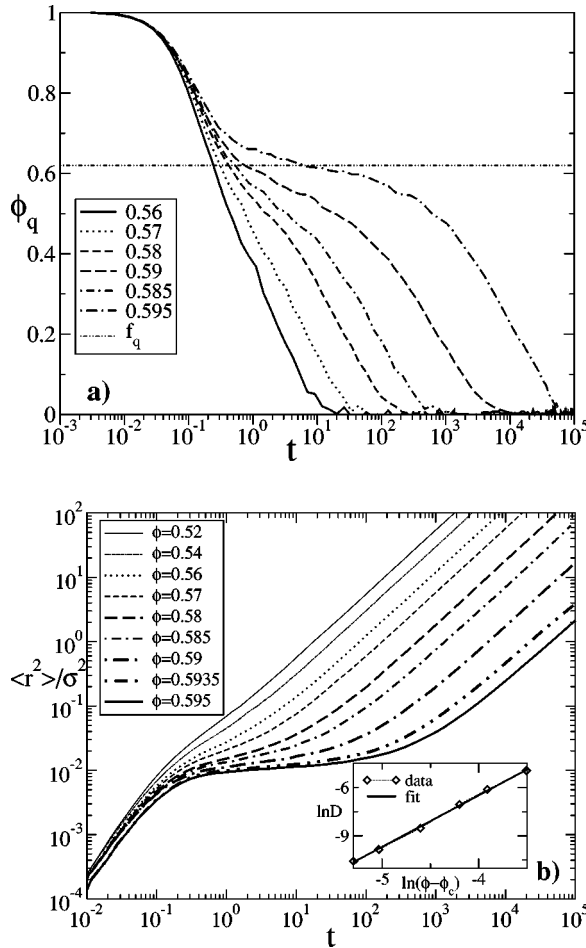


FIG. 5. (a) Normalized density-density correlators along the isotherm $T=2.0$ for different packing fractions in function of time. Time units, as specified in the text, are $\sigma_B(m/u_0)^{1/2}$. The q vector displayed in this picture, and in all the following ones if not differently specified, is slightly larger than that for the first peak of the static structure factor, and it corresponds to the value $q=25$ in units of half the box size (π/L). The horizontal line represents the corresponding nonergodicity parameter, as extrapolated from the fit (see text). (b) Mean-square displacement along the isotherm $T=2.0$ for the same densities as in (a). In the inset we plot $\ln D$ vs $\ln(\phi - \phi_c)$ to show the power-law behavior described in Eq. (8) for our data. With such a fit we can evaluate the MCT exponents, as explained in the text. Note that $\phi_c=0.60$ is also a parameter of the fit.

uncertainty on the exponent is due to the variation it gets when considering only the points closest to the transition. We note that in Ref. [8], the case reported brings a value of $\gamma = 3.03$. Thus, we are, at this value of temperature, already in a situation much closer to a higher order singularity, corresponding to other MCT exponents, obtained by means of Eqs. (10) and (9), respectively, $b=0.41 \pm 0.07$ and $\lambda=0.84 \pm 0.04$. It is perhaps important to stress at this point that the value of γ obtained with this procedure can be slightly wrong due to the difficulty of getting close enough to the ideal glass transition with numerical simulations [44]. We will use the so-calculated value of b in the following to fit the behavior of density correlators along the isodiffusivity

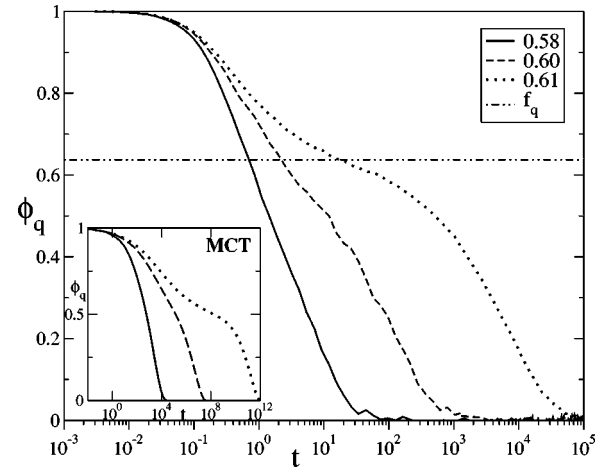


FIG. 6. Same as in Fig. 5(a) for $T=0.75$. The reported densities in this case have been chosen to evidence the analogy with the MCT predictions of Fig. 11 in Ref. [4], reproduced in the inset for comparison.

curve $D/D_0=5 \times 10^{-6}$, to give an idea of the behavior of quantities of interest along the ideal glass transition line.

We do not show here the behavior of density correlators and MSD for the case $T=1.5$, because its results are completely analogous to $T=2.0$. We note, however, that the fit of the diffusivity with Eq. (8) gives in this case the exponents $\gamma=3.6 \pm 0.4$, $b=0.35 \pm 0.05$, and $\lambda=0.87 \pm 0.04$. The increase in the value of λ is expected since we are getting closer to the reentrant region, and consequently to the singularity. The same trend is observed for $T=1.0$ with γ still increasing up to about 3.9 ± 0.3 , and λ reaching the value of 0.89 ± 0.02 .

At $T=0.75$ an interesting behavior appears. Indeed, in the density correlators, a logarithmic decay starts to emerge. As shown in Fig. 6, some state points display a logarithmic decay (see curve for $\phi=0.58$ in the figure) for almost the whole relaxation process, i.e., after the microscopic relaxation up to complete decay. The shape of this logarithmic behavior appears quite different from that found in Ref. [8]. On the other hand, it resembles quite closely the shape of MCT correlators near the A_3 singularity for the 3% square-well potential reported in Fig. 11 of Ref. [4], which for comparison is reported in the inset in Fig. 6. Upon increasing density, and so getting closer to the glass transition, the relaxation changes to the usual two-step form, clearly indicating a similar situation of our isothermal path to that indicated in the inset of Fig. 11 cited above. Thus, the higher order singularity dominates the dynamics at smaller packing fractions, but when one gets sufficiently close to the glass transition, a conventional A_2 singularity is met, and this causes the restoration of the typical α relaxation. By considering only those packing fractions, when at least the beginning of the α relaxation can be observed (i.e., $\phi > 0.6$), we can fit the diffusivity again with Eq. (4), obtaining the extremely high, but very rough, value $\gamma \sim 5.1$, corresponding to the value of $b \sim 0.25$ and $\lambda=0.937$, thus considerably getting closer to the value 1 corresponding to the A_3 point. We cannot estimate here the error due to the small number of points

available (only five for three parameters for the fit). However, even if not so precise, it clearly gives a strong indication that we are approaching a higher order singularity. We recall here that the topology of the transition, as predicted by the theory (see inset of Fig. 4), is such that the higher order singularity of type A_3 lies inside the glass region, so that by studying the diffusivity going to zero one can at most reach the boundary of the glassy region, i.e., the most reentrant point in the phase diagram. Thus, the study of the behavior of the exponents approaching the glass line gives a strong indication of the presence and location of the higher order singularity in the present system, although one needs further evidence as, for example, from analyzing the nonergodicity factors, as we shall do later, to claim the presence of two distinct types of glasses, and thus to establish undoubtedly the existence of a transition point between them, that is, the A_3 singularity in the theoretical treatment. Thus, for example, by looking at the shape of the nonergodicity factor below, we can anticipate that at this temperature we are meeting the A_2 line along its repulsive branch, again as in the inset of Fig. 11 of Ref. [4], but probably at a slightly higher temperature.

From these considerations, it emerges that this scenario can be considered the typical one as predicted by MCT, for the interplay between an A_2 -repulsive singularity and a higher order one, i.e., A_3 . It is indeed closely connected to the asymptotic calculations performed in Ref. [15] for the two-component schematic model whose results are reported there in Fig. 9.

Now we turn to the case $T=0.6$. The correlators, reported in Fig. 7(a), show an even closer behavior to that predicted by MCT in Ref. [4] (again Fig. 11 in Ref. [4], i.e., inset of Fig. 6 here). However, at this temperature, the two competing singularities must be so close to each other that a clear α relaxation does not take place within the reach of our simulation, i.e., the logarithmic behavior remains always very important, and even at higher packing fractions it is clearly observable before the α process takes over. The interesting feature emerging is that, in all the cases considered, the logarithmic behavior never extends for much more than 3.5 decades in time. This arises because, in the present topology of the phase diagram, one is either too close to the A_2 singularities to observe a pure logarithm, or too far from the glass transition, and thus the relaxation time is generally not too large. Indeed, this behavior is strongly supported again by the theoretical calculations in Ref. [4].

It should be noted that at this temperature we are not able to convincingly fit the power-law density dependence of the diffusivity. Indeed, if one forces the fit on the points, one finds exponents strongly dependent on the selected ϕ range. A possible explanation for this data sensitivity to ϕ can be found in the competition between A_2 - and A_3 -dominated dynamics. In such a condition, only a comparison with a full MCT solution (as opposed to an asymptotic prediction) may help in rationalizing the density dependence of diffusivity. In agreement with the previous observations, also the MSD, represented in Fig. 7(b), starts to show deviations from the usual A_2 -type behavior for a discontinuous transition. Indeed, a clear flat region does not appear, though the dynam-

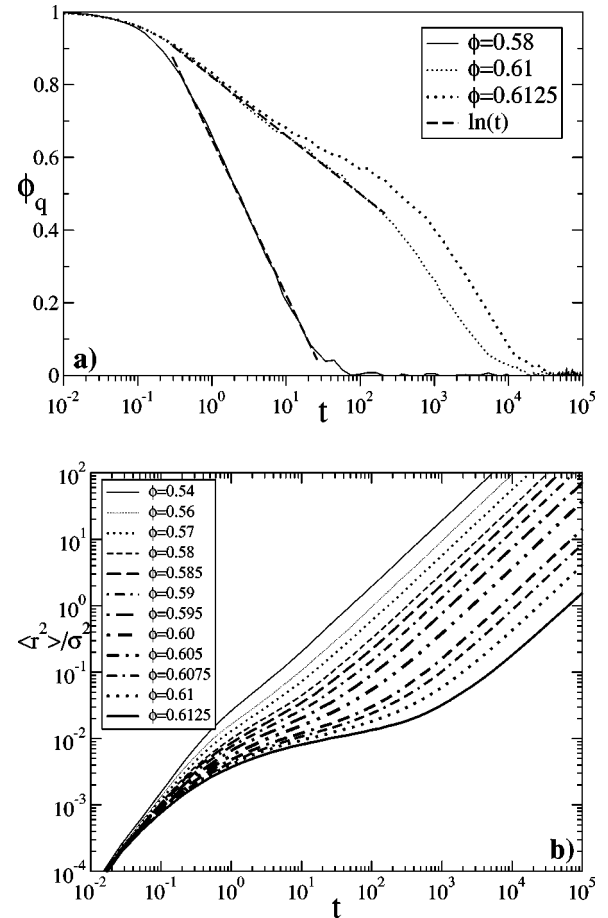


FIG. 7. (a) Same as in Fig. 5(a) for $T=0.6$. The dashed lines represent fits with logarithmic laws, which are displayed to show the presence of a logarithmic decay and the mechanism of its disappearance in the proximity of an A_2 singularity (see text for further details). They are reported as a guideline to the eye, and not to extrapolate any fit parameters. (b) As in Fig. 5(b) for $T=0.6$.

ics is significantly slow. What can be observed is a slight deviation from the flat region at higher temperatures, which will become more and more evident at lower temperatures. No clear localization length can be found. Attraction at this temperature has become quite relevant. It is again a sign of very strong competition between different singularities, between attractive and repulsive cages.

Upon further decreasing temperature, we enter the most delicate region of the phase diagram. Indeed at $T=0.5$, as for $T=0.6$, it is not possible to find any MCT exponents, and the interpretation of the behavior of the correlators is not straightforward. These are plotted in Fig. 8(a). Indeed, at higher densities there is evidence of some logarithmic behavior, but no clear development of a plateau ever takes place. This might be due to the fact that, since we are approaching more closely the attractive branch of the glass transition by examining a lower temperature, the plateau should be higher and the interplay of the two types of singularities would be different than what was observed previously. Thus, we can interpret this behavior as one dominated by an A_2 -attractive and an A_3 singularity, similar again to what was shown in the

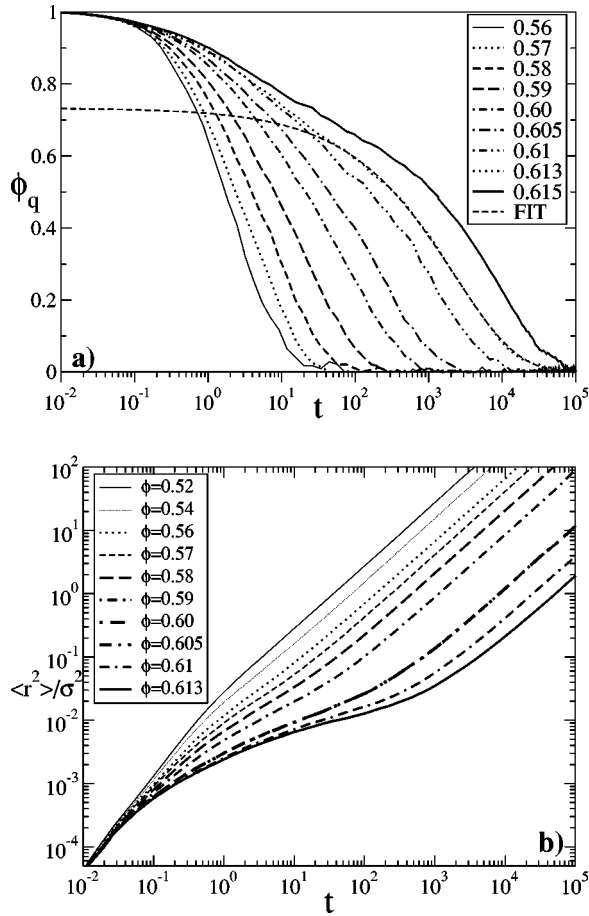


FIG. 8. (a) As in Fig. 5(a) for $T=0.5$. The dashed line is a fit of one of the correlators with a stretched exponential, whose extrapolated parameters [see Eq. (5)] are $\beta_q \approx 0.5, \tau_q \approx 2.2 \times 10^3, A_q \approx 0.73$, the last one giving an estimate for the nonergodicity parameter f_q , and it is shown to display the quality of the fit. Parameters of the stretched exponential fits as a function of the wave vector are reported in Fig. 9. (b) As in Fig. 5(b) for $T=0.5$.

analytical calculations of Ref. [15], there presented in Fig. 5 (curves labeled as $n'=2,3$).

We note, however, that the long-time decay of density correlators can be represented by a stretched exponential, but with very low exponents β_q , as shown in Fig. 9. In the MSD, reported in Fig. 8(b), the phenomenon present at the previous temperature becomes more accentuated. Even the slowest studied state point is far from being asymptotic, and the MSD presents a clear transient region.

The case where the anomalous dynamics and the interplay between different singularities is fully displayed is offered by the $T=0.4$ isotherm. The correlation functions, shown in Fig. 10(a), are rather peculiar. Even the long-time limit is far from being rationalized in terms of stretched exponential decay. The MSD behavior, shown in Fig. 10(b) is also quite intriguing. The MSD transient behavior is now evidently of a subdiffusive type. Indeed, for about 4 decades in time, it shows a dependence which can be quite accurately described by a power-law behavior, i.e.,

$$\langle r^2 \rangle \sim t^x. \quad (11)$$

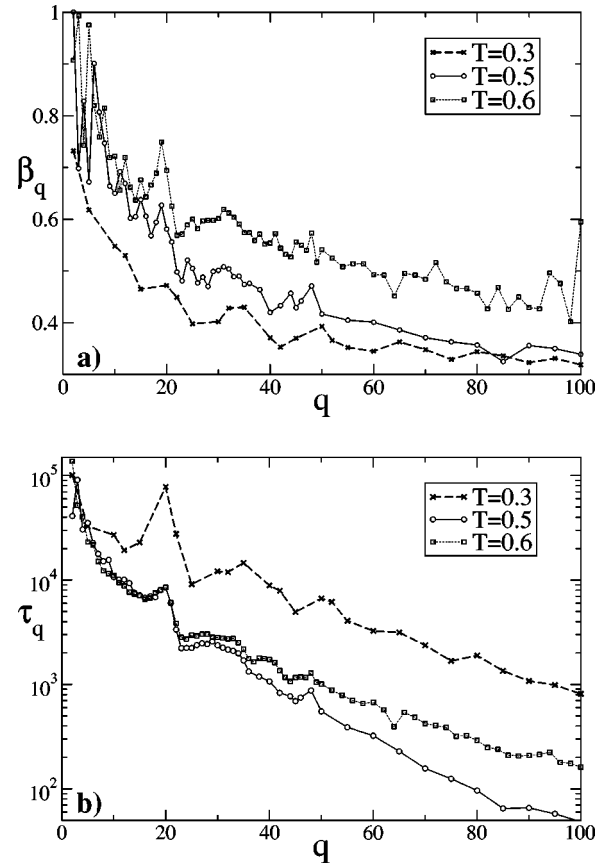


FIG. 9. (a) Exponent β_q as a function of q (always in units of half the box size π/L) obtained from the fit of the density-density correlation function with the stretched exponential in Eq. (5) for temperatures $T=0.6, 0.5, 0.3$. The values found are always very small, indicating a very slow relaxation. (b) As in (a) for the relaxation time parameter τ_q of Eq. (5). Interestingly, a peak corresponding to the q value of the first peak of the static structure factor emerges (i.e., $q \sim 20$), as one lowers the temperature.

We estimated via a fit $x \approx 0.44$. A similar behavior has been found in the MCT study of polymeric systems [45], for displacements varying from the typical localization length of hard-sphere-like cages to end-to-end distance. The analogy with the polymeric systems, where permanent bonds are present (in a sense close to the attractive cages at this very low temperature), can be a guide to a deeper understanding of this region.

The strong effects that we find at this value of temperature seem to suggest that along this isotherm the system approaches the closest point to the singularity, even if we do not know yet on which side (attractive or repulsive) of the glass line it will be located. To understand the nature of the dynamics which takes place here, further investigations are needed, as well as a more complete analysis of the correlators, and a comparison with full solutions of the MCT equations.

Finally we analyze the last isotherm, corresponding to $T=0.3$. This being a very low value for the system to equilibrate, data are not so clean as for the other cases, also because here one needs to study slower points with respect to the other temperatures in terms of bare diffusivities, to reach

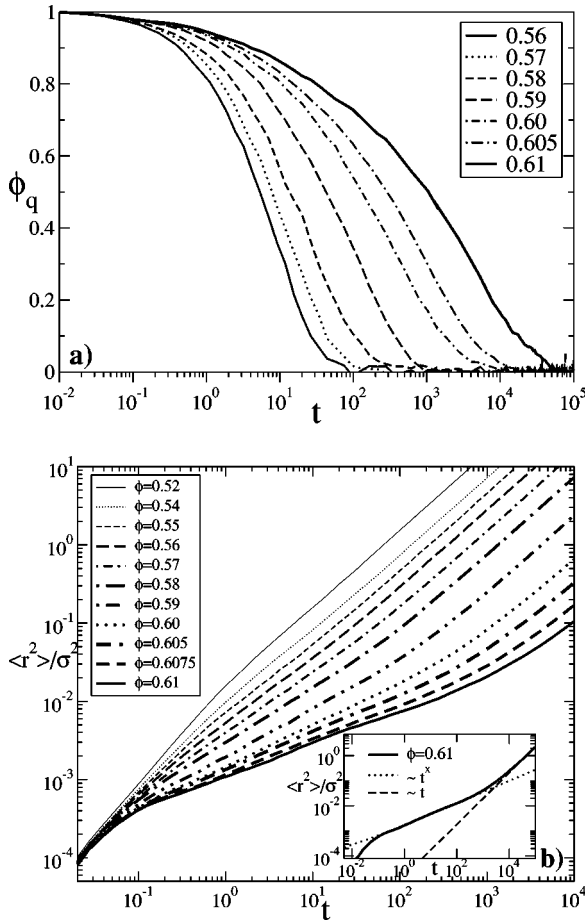


FIG. 10. (a) As in Fig. 5(a) for $T=0.4$. (b) As in Fig. 5(b) for $T=0.4$. In the inset the fit of the subdiffusive and diffusive regimes with a power law are shown (see text for details).

the same values of normalized ones. However, despite these technical difficulties, we find more transparent results in terms of conventional MCT interpretations, i.e., we can identify the development of a two-step process typical of an A_2 singularity, both for the correlators and for the MSD than in the previous case.

Indeed, observing the correlators in Fig. 11(a), it is clear that, close enough to the transition, they present the development of a plateau, and thus, an α -relaxation process, as shown in the inset of the figure for various q vectors. Despite this clear behavior, even at this temperature, it is not possible to evaluate unambiguous power-law exponents from the diffusivity, but stretched exponential fits give reasonable results. Thus, the value of the plateau is found to be extremely high. We remind the reader that one of the key experimental observations in the slow dynamics of colloidal systems was the unusual very high value of the plateau [46]. This is also what has been found within MCT as a quantitative distinction between attractive and repulsive glasses, leading, for example, to very different mechanical properties for the two glasses [5]. This allows us to say that we here have a clear indication that, at this low temperature, we are approaching the glass transition from the attractive glass side. It is also of deep interest to note the analogy of this behavior with the one that has been found in the study of “strong” gels [47],

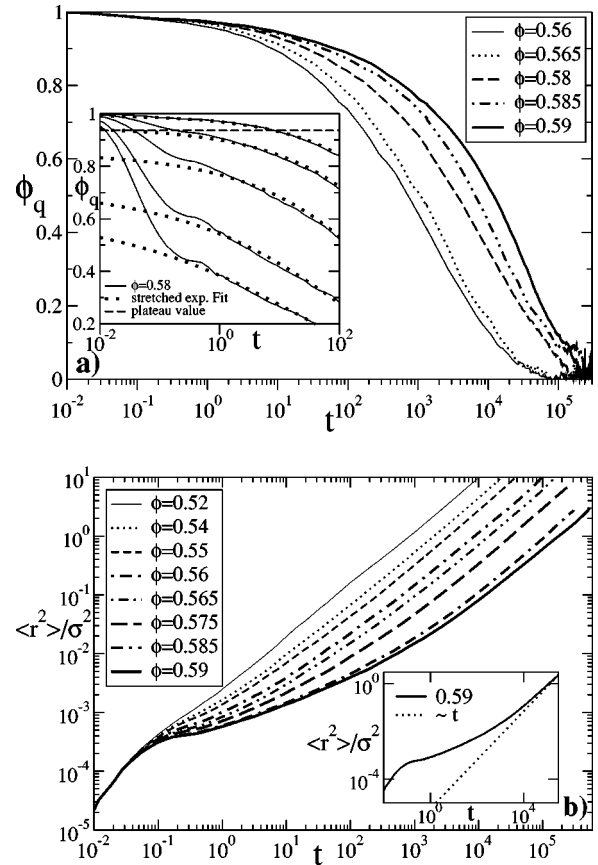


FIG. 11. (a) As in Fig. 5(a) for $T=0.3$. In the inset data and stretched exponential fits are shown for different q values at the same packing fraction $\phi=0.58$. In particular, starting from the upper correlator, they correspond, respectively, to $q = 25, 55, 95, 155, 205$ in units of π/L . This is done in order to make more evident the presence of a plateau in the relaxation, which is also drawn in the figure for the case $q=55$. (b) As in Fig. 5(b) for $T=0.3$. In the inset a fit as in Fig. 10(b) is shown. There is no evident subdiffusive regime.

even if this should be inspected at lower densities also.

Figure 11(b) represents the evolution of MSD at this temperature. Here, a signature of a localization length, much smaller than that found in the high temperature cases, starts to develop. Indeed, an indication of a plateau is observable around $\langle r^2 \rangle = 0.0006\sigma^2$. The corresponding localization length is of the order of Δ , supporting the interpretation that at this temperature the relevant localization length has become the attractive well. In this respect, one can interpret the subdiffusive behavior of the MSD discussed at $T=0.4$ as a crossover effect between the different localization lengths, i.e., the hard-sphere (repulsive) typical distance and the attractive well. In theoretical terms, this is due to the two distinct A_2 singularities, corresponding to repulsive and attractive glass transitions, while in the polymeric case [45] there is only one A_2 singularity. We might argue that there the bonding of the polymers is taking the place of the attractive transition in our system, originating the same effect of slower intermediate diffusivity when both these two competing mechanisms are strongly present.

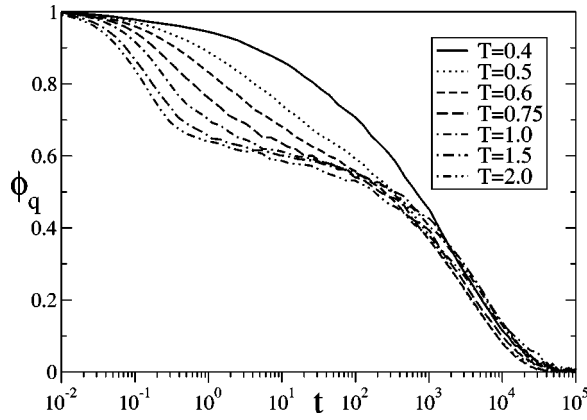


FIG. 12. Density-density correlation function along the iso- D/D_0 line, $D=5\times 10^{-6}$. The wave vector chosen corresponds for all cases to $q=25$ in units of half the box size.

V. RESULTS: ALONG THE ISO- D/D_0 CURVE

We now focus on studying the behavior of correlators and MSD, and other quantities along the iso-(normalized)-diffusivity, i.e., the iso- D/D_0 , curve; $D/D_0=5\times 10^{-6}$, shown in Fig. 4, which represents our closest available representation of the ideal glass transition line. The aim of this study is to give clear evidence of the existence of two distinct glassy states, attractive and repulsive. Also, it aims to connect even more closely this simulation to the MCT calculations, which also were performed in a similar fashion, along the ideal glass lines, in Ref. [5].

We start by representing the behavior of density correlators along the iso- D/D_0 line in Fig. 12. The curves here represented, having equal diffusivity, also have the same normalized relaxation time. Thus, we can clearly see the change in the decay that takes place, upon decreasing temperature, from a marked α relaxation at higher temperature to the extremely slow decay of $T=0.4$, passing through the intermediate regimes between $T=0.75$ and $T=0.5$. Here, the only evident logarithmic behavior can be observed for $T=0.6$ and $T=0.5$, because these must be the only cases for which the proximity to the A_2 transition strongly competes with the close A_3 singularity, as discussed above.

Next, we report the MSD behavior along the line in Fig. 13. Despite the larger statistical error at $T=0.3$, we display this case also as an important part of the whole picture. Thus, here, we can clearly observe the change in the diffusion process. The first evident thing to note is the big gap, of about ≈ 1.5 orders of magnitude, in the plateau values corresponding to high and low temperatures. This implies a factor of about 7 in the ratio of the localization lengths of the particles, which, as discussed above, characterizes the size of cages around particles. Clearly this result can be used as a justification to speak of “attractive” cages, opposed to normal cages, intended as a simple occupation of the available space. In the attractive cages, the average distance between particles is much smaller, the lower the temperature. This is a clear signal of a different structure in the glass formation.

Also, we can examine more carefully the modification of the plateau present at higher temperatures in the transient

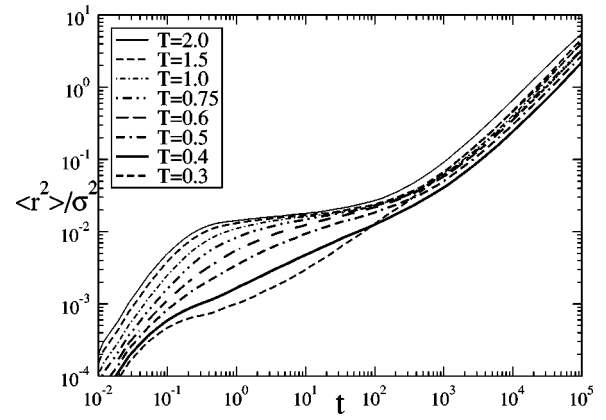


FIG. 13. Mean-square displacement along the iso- D/D_0 line, $D=5\times 10^{-6}$. The line for $T=0.3$ crosses lines for higher T due to large statistical errors in determining D at such low temperature.

regime. Indeed, increasing the attraction, this tends to bend downwards until a sort of “saturation” between the two competing mechanisms (attraction and packing) takes place, corresponding to the subdiffusive behavior of $T=0.4$. After this point, attractions become dominant, and the curve starts to bend upwards. This might suggest that, going to even lower diffusivities, the MSD would display a similar plateau as for high temperatures at roughly $\langle r^2 \rangle \sim 0.0007\sigma^2$ [48], which means roughly a localization length of 2.6% of the particle diameter, i.e., comparable with the width of the attractive well of the model, confirming our conjectures on the formation of attractive cages, or, to use another expression, bonds. However, to gain further evidence on how these mechanisms really happen and evolve in the system, a specific study of configurations in terms of average distance, sizes of clusters, and heterogeneities, in general, should be performed, and this is beyond the scope of the present work. We note that a similar figure, showing the behavior of MSD with attraction, has appeared in [9], but not all of these considerations could be made there, due to the distance from the transition.

We now turn to evaluate the nonergodicity factor f_q along the iso- D/D_0 curve. To do this, we have fitted the density correlators at various q vectors, and extracted the relevant parameters. Where possible, i.e., where the power-law behavior for the diffusivity in Eq. (8) was found to be valid, we used the power-law described in terms of the b exponent for the α relaxation of Eq. (4). Thus, for $T=2.0$, we implemented the fit with $b=0.41$, while for $T=1.5, 1.0$, and 0.75 we used $b=0.35, 0.31$, and 0.25 , respectively. These values have been found very good for the fits, always finding a χ^2 of the order of 10^{-4} or less. For lower temperatures, it was not possible to use this strategy and, consequently, we used the approach of the stretched exponential in Eq. (5), and use its amplitude as an estimate for f_q . The parameters of the fits, i.e., the exponent of the stretching β_q and the relaxation time τ_q , for the considered temperatures $T=0.6, 0.5, 0.3$ are reported in Fig. 9 to display their q behavior. Even though the stretched exponential law is not analytically justified, it is quite well established in the literature to use as a fitting law for extracting the nonergodicity parameter [44]. In the case

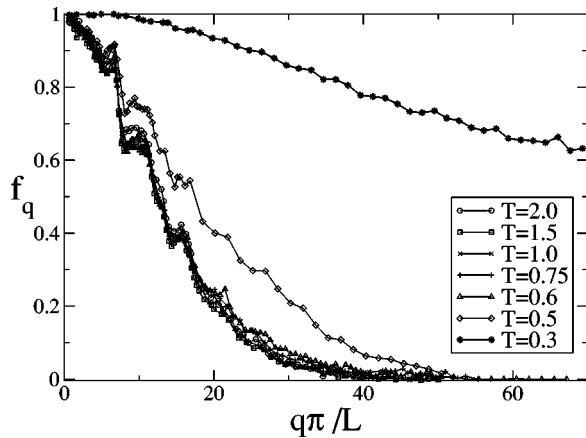


FIG. 14. Nonergodicity parameter f_q as a function of $q\pi/L$ along the iso- D/D_0 line, $D=5 \times 10^{-6}$, as obtained by fitting the correlation functions (see text for details). It is evident how all the data collapse onto each other for all temperatures less than 0.6, giving a clear indication of a repulsive glass, while for lower temperatures f_q increase quite dramatically towards typical attractive glass behavior [5].

of $T=0.4$ also this strategy did not work, as already discussed [49].

In Fig. 14 we show the so-calculated f_q . Amazingly, from $T=2.0$ down to $T=0.6$, they all collapse onto the same curves, giving a strong evidence of MCT predictions for the repulsive glass [5]. Thus, the repulsive glass is independent of temperature, and also this shows how the passage to attractive glass intervenes quite sharply. For lower temperatures, the glass becomes attractive, and the nonergodicity parameter starts to be modified with temperature, becoming finite also at much larger q vectors [5]. Despite some errors generated by the stretched exponential fits at these low temperatures or the data noise at $T=0.3$, a significant change in the shape and width of f_q is seen between $T=0.5$ and $T=0.3$. It could be that the case at $T=0.5$ is quite sensitive to the singularity, and thus it is a somehow intermediate case. A more detailed study, either theoretically or by considering intermediate or even lower temperatures for smaller packing fractions, will be helpful for clarifying this issue. On the other hand, the establishment of the existence of the two glasses along the line appears to be definite by these results. To support this statement, we have plotted in Fig. 15 both the (partial) static structure factor $S_{AA}(q)$ (rescaled by a factor of 2 for having a better visualization of the figure) and the nonergodicity factor, respectively, at the highest, $T=2.0$, and at the lowest, $T=0.3$, temperatures studied in this work, so as to compare the most extreme cases of repulsive and attractive glasses. First, we note how the oscillations of the nonergodicity factors follow these in the structure factor quite closely in both cases, even though for the $T=0.3$ case it is actually quite difficult to visualize these [50]. Also, the $S(q)$ presents the typical features we expected from theoretical calculations within MCT and the integral equations. Indeed, the repulsive case shows a marked first peak, which is the main responsible for the glass transition, while the attractive one possesses larger secondary oscillations, which constitute

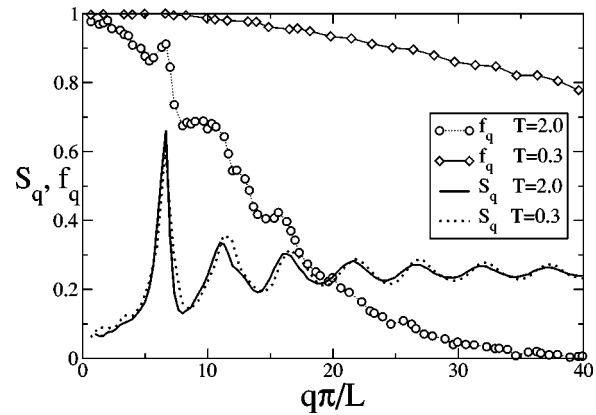


FIG. 15. Nonergodicity parameter f_q and partial static structure factor S_q at $T=2.0$ and $T=0.3$. The different shape of f_q reflects the difference between attractive and repulsive glass (see text for details).

a signal of the smaller cages already described above. Thus, this contributes to establish not only the existence of the two glasses, but also, and most importantly, the two distinct mechanisms which drive the glassification in the two cases, i.e., simply packing and localized attraction.

VI. CONCLUSIONS

In this paper, using molecular dynamics, we have studied the dynamical arrest phenomena of spherical particles interacting via a square-well potential. The square-well potential has been studied as one of the simplest canonical models of solids, liquids, and gases for many years [22–27]. Here we have extended the models' applicability to the domain of dynamical arrest and glassy phenomena. Previous predictions for dynamical arrest from the mode-coupling theory for the square-well potential are available [4,5], so direct comparisons are feasible.

By using a well-adjusted binary mixture, we have been able to extend our previous preliminary investigations [21] much closer to the arrest transition, accessing diffusion constants that are three orders of magnitudes smaller than in the previous calculations. Nevertheless, results on the lowest valued isodiffusivity curve available for the single-component system are very close to those for the binary mixture, so we may consider the role of the second component to be mainly the prevention of crystallization.

In that regime where repulsions dominate, we recover an ideal glass transition with power-law scaling of the diffusion constant. We also find an attractive branch to the dynamical arrest where theory has predicted the presence of an attractive glass. Where attractions and repulsions compete in nearly equal terms we find reentrance in the arrest curves when plotted in units of the microscopic temperature dependence of the diffusion constant. However, fixed-density diffusion constants, plotted without any normalization, exhibit a maximum in the diffusion constant as the temperature is increased. This maximum locates the reentrant liquid where mobility is anomalously high. We consider the essential features of reentrance in this regime for the square-well poten-

tial now to be confirmed, in agreement with the predictions of theory [4].

We have studied also the evolution of the density-density correlation functions (dynamical structure factors) and, independently, the mean-squared distance traveled by particles in the vicinity of the reentrant regime. As expected, where repulsive interactions dominate, we find the classical arrest scenario in which plateaus develop in both functions as arrest is approached [16]. These plateaus indicate the development of an observable characteristic cage time, and are quite typical of prediction by MCT for hard-sphere systems. When attraction begins to compete on equal terms, in the vicinity of the reentrant regime, the theory has predicted the existence of an A_3 singularity embedded in the arrested region. It is therefore difficult to access this singularity directly by molecular dynamics, but the theory has indicated that there are distinctive signatures of this singularity in the reentrant fluid phase, on approach to arrest. In particular, density correlators from a suitable fixed-temperature cut of the phase diagram have an interesting pattern of behavior in which the logarithmic behavior [15], due to the embedded A_3 point, first begins to dominate, and then crosses over to the conventional A_2 , either repulsive or attractive, behavior more commonly observed for normal MCT arrest. The density correlators in the reentrant regime clearly exhibit this phenomenon, the pattern of evolutions being essentially in agreement with the predictions of theory.

We may pause here to comment that we do not regard this complex crossover behavior as a complication, but in fact as a rather delicate and unusual signature of the whole reentrant phenomenon, and an interplay between A_2 and A_3 singularities. That the simulations would reproduce this is strong support for the detailed picture offered by theory. The behaviors of the mean-squared displacements are also quite unusual, and there is as yet no theoretical prediction for them in this regime.

Finally, we are able to extract the nonergodicity factors along the arrest curve, for the lowest iso-(normalized)-diffusivity constant curve. Again, in line with theoretical predictions, we find strong evidence of a transition from a re-

pulsive glass to attractive glass behavior, as indicated by the change in the characteristic shapes of the nonergodicity factors. This is a direct evidence of the repulsive glass to attractive glass transition that has been predicted by the theory, representing one of the most remarkable phenomena associated with the system.

The theory suffers from strong systematic shifts of all the arrest curves in relation to the simulated ones, a phenomenon long known from the example of the hard sphere. However, qualitatively, the theoretical predictions of the reentrant regime, with an associated crossover to logarithmic singularity, and glass-to-glass transition has been confirmed by detailed molecular dynamics calculations.

From the experimental point of view, there is accumulated evidence that all the phenomena described here are robust, being relatively independent of the details of the experimental system used to study them [17–19,9]. The same is true of the theoretical studies [1,2,4–7] and simulations [8,21]. The square-well potential is one of the simplest examples one can study, and it is reassuring that it exhibits the phenomena.

Our original prediction that in the dense regime, a colloidal particulate system with short-ranged potentials could be described using ideas from dynamical arrest and glass theory now seems to be strongly supported. Dense particle gels are thereby identified as an example of a type of glass, or dynamically arrested phase. The implications are broader than the simple example studied, for it indicates that it may be possible to interpret many formerly disparate phenomena such as coagulation, precipitation, aggregation, and gellation within the paradigm of dynamical arrest or glass theory. This is a fundamental sort of perception in the field of dense soft-condensed matter, which may prove to be very fruitful in coming years.

ACKNOWLEDGMENTS

We thank W. Götze, M. Fuchs, and W. Kob for interesting comments. This research is supported by the INFM-HOP-1999, MURST-PRIN-2000, and COST PI. S.V.B. thanks the University of Rome *La Sapienza* and NSF, Chemistry Division (Grant No. CHE0096892) for support.

-
- [1] J. Bergenholtz and M. Fuchs, *Phys. Rev. E* **59**, 5706 (1999).
 - [2] L. Fabbian, W. Götze, F. Sciortino, P. Tartaglia, and F. Thiery, *Phys. Rev. E* **59**, R1347 (1999); **60**, 2430 (1999).
 - [3] G. Foffi, E. Zaccarelli, F. Sciortino, P. Tartaglia, and K.A. Dawson, *J. Stat. Phys.* **100**, 363 (2000).
 - [4] K.A. Dawson, G. Foffi, M. Fuchs, W. Götze, F. Sciortino, M. Sperl, P. Tartaglia, Th. Voigtmann, and E. Zaccarelli, *Phys. Rev. E* **63**, 011401 (2000).
 - [5] E. Zaccarelli, G. Foffi, K.A. Dawson, F. Sciortino, and P. Tartaglia, *Phys. Rev. E* **63**, 031501 (2001).
 - [6] G. Foffi, G.D. McCullagh, A. Lawlor, E. Zaccarelli, K.A. Dawson, F. Sciortino, P. Tartaglia, D. Pini, and G. Stell, *Phys. Rev. E* **65**, 031407 (2002).
 - [7] K.A. Dawson, G. Foffi, G.D. McCullagh, F. Sciortino, P. Tartaglia, and E. Zaccarelli, *J. Phys.: Condens. Matter* **14**, 2223 (2002).
 - [8] A.M. Puertas, M. Fuchs, and M.E. Cates, *Phys. Rev. Lett.* **88**, 098301 (2002).
 - [9] K.N. Pham, A.M. Puertas, J. Bergenholtz, S.U. Egelhaaf, A. Moussaid, P.N. Pusey, A.B. Schofield, M.E. Cates, M. Fuchs, and W.C.K. Poon, *Science* **296**, 104 (2002).
 - [10] K.A. Dawson, *Curr. Opin. Colloid Interface Sci.* **7**, 218 (2002).
 - [11] E. Zaccarelli, F. Sciortino, P. Tartaglia, G. Foffi, G.D. McCullagh, A. Lawlor, and K.A. Dawson, *Physica A* **314**, 538 (2002).
 - [12] R.J. Baxter, *J. Chem. Phys.* **49**, 2770 (1968).
 - [13] U. Bengtzelius, W. Götze, and A. Sjölander, *J. Phys. C* **17**, 5915 (1984).
 - [14] W. Götze, in *Liquids, Freezing and Glass Transition*, edited by J.P. Hansen, D. Levesque, and J. Zinn-Justin (North-Holland, Amsterdam, 1991), p. 287.
 - [15] W. Götze and M. Sperl, *Phys. Rev. E* **66**, 011405 (2002).

- [16] W. Götze, *J. Phys.: Condens. Matter* **11**, A1 (1999).
- [17] E. Bartsch, M. Antonietti, W. Shupp, and H. Sillescu, *J. Chem. Phys.* **97**, 3950 (1992); E. Bartsch, V. Frenz, J. Baschnagel, W. Schärtl, and H. Sillescu, *ibid.* **106**, 3743 (1997); A. Kasper, E. Bartsch, and H. Sillescu, *Langmuir* **14**, 5004 (1998).
- [18] T. Eckert and E. Bartsch, *Phys. Rev. Lett.* **89**, 125701 (2002).
- [19] F. Mallamace, P. Gambadauro, N. Micali, P. Tartaglia, C. Liao, and S.H. Chen, *Phys. Rev. Lett.* **84**, 5431 (2000).
- [20] E.B. Brauns, M.L. Madaras, R.S. Coleman, C.J. Murphy, and M.A. Berg, *Phys. Rev. Lett.* **88**, 158101 (2002).
- [21] G. Foffi, K.A. Dawson, S.V. Buldyrev, F. Sciortino, E. Zaccarelli, and P. Tartaglia, *Phys. Rev. E* **65**, 050802 (2002).
- [22] B.J. Alder, D.A. Young, and M.A. Mark, *J. Chem. Phys.* **56**, 3013 (1972).
- [23] M.G. Noro and D. Frenkel, *J. Chem. Phys.* **113**, 2941 (2000).
- [24] J.R. Elliot and L. Hu, *J. Chem. Phys.* **110**, 3043 (1999).
- [25] L. Vega, E. de Miguel, L.F. Rull, G. Jackson, and I.A. McLure, *J. Chem. Phys.* **96**, 2296 (1996).
- [26] J. Chang and S.I. Sandler, *Mol. Phys.* **81**, 745 (1994).
- [27] C. Rascon, L. Mederos, and G. Navascues, *Phys. Rev. Lett.* **77**, 2249 (1996).
- [28] Note an error in Ref. [21] where all the reported values for the diffusivity were to be divided by the factor 6, by using Eq. (7).
- [29] S. Torquato, T.M. Truskett, and P.G. Debenedetti, *Phys. Rev. Lett.* **84**, 2064 (2000).
- [30] K.A. Dawson, G. Foffi, F. Sciortino, P. Tartaglia, and E. Zaccarelli, *J. Phys.: Condens. Matter* **13**, 9113 (2001).
- [31] D.C. Rapaport, *The Art of Molecular Dynamic Simulation* (Cambridge University Press, Cambridge, 1995).
- [32] E. Zaccarelli, G. Foffi, F. Sciortino, P. Tartaglia, and K.A. Dawson, *Europhys. Lett.* **55**, 139 (2001).
- [33] E. Zaccarelli, P. De Gregorio, G. Foffi, F. Sciortino, P. Tartaglia, and K.A. Dawson, *J. Phys.: Condens. Matter* **14**, (2002).
- [34] T. Franosch, W. Gtze, M.R. Mayr, and A.P. Singh, *J. Phys.: Condens. Matter* **71**, 235 (1998).
- [35] J.P. Hansen and I.R. McDonald, *Theory of Simple Liquids* (Academic Press, London, 1986).
- [36] W. Götze and R. Haussmann, *J. Phys. B* **72**, 403 (1988).
- [37] W. van Meegen and S.M. Underwood, *Phys. Rev. Lett.* **70**, 2766 (1993); *Phys. Rev. E* **49**, 4206 (1994).
- [38] P. Bolhuis and D. Frenkel, *Phys. Rev. Lett.* **72**, 2211 (1994); P. Bolhuis, M. Hagen, and D. Frenkel, *Phys. Rev. E* **50**, 4880 (1994).
- [39] A. Scala, F.W. Starr, E. La Nave, F. Sciortino, and H.E. Stanley, *Nature (London)* **406**, 166 (2000).
- [40] J.L. Barrat, W. Götze, and A. Latz, *J. Phys.: Condens. Matter* **1**, 7163 (1989).
- [41] N.W. Ashcroft and N.D. Mermin, *Solid State Physics* (Fort Worth, London, 1976).
- [42] W. Kob and H.C. Andersen, *Phys. Rev. E* **52**, 4134 (1995).
- [43] W. Götze and M. Sperl (private communication).
- [44] M. Nauroth and W. Kob, *Phys. Rev. E* **55**, 657 (1997); A. Rinaldi, F. Sciortino, and P. Tartaglia, *ibid.* **63**, 061210 (2001).
- [45] S.-H. Chong and M. Fuchs, *Phys. Rev. Lett.* **88**, 185702 (2002).
- [46] H. Verduin and J.G.K. Dhont, *J. Colloid Interface Sci.* **172**, 425 (1995).
- [47] E. Del Gado, L. De Arcangelis, and A. Coniglio, e-print condmat/0209478.
- [48] We note that this value is slightly higher than that one observed in Fig. 11(b), because here we are looking at a point slightly less close to the glass transition; thus localization is a bit less effective for this case. However, whenever localization due to attractive glass transition happens, the value of the MSD at the plateau is always smaller than $\Delta^2=0.0009\sigma^2$.
- [49] We note that, by using the stretched exponential law, a good fit of the correlators can be obtained. However, the parameters that are found from the fits are completely unreliable. In particular, for the amplitude parameter, which should give an estimate of the nonergodicity parameter, we find for every q vector, the value 1. Thus, we must exclude the validity of these fits.
- [50] This is due to the fact that at $T=0.3$, and in general for attractive glasses, the nonergodicity factor decays extremely slowly, and it is not possible to do so within the present figure. However, the oscillations might be more evident in Fig. 14 even at this temperature.